California State University, San Bernardino

CSUSB ScholarWorks

2008

Characterization of natural spring waters of the San Bernardino Mountains using stable isotopes of oxygen and hydrogen

Alison Renee Sloat

Follow this and additional works at: https://scholarworks.lib.csusb.edu/etd-project

Part of the Hydrology Commons

CHARACTERIZATION OF NATURAL SPRING WATERS OF THE

SAN BERNARDINO MOUNTAINS USING STABLE

ISOTOPES OF OXYGEN AND HYDROGEN

_____

A Project

Presented to the

Faculty of

California State University,

San Bernardino

_____

In Partial Fulfillment

of the Requirements for the Degree

Master of Science

in

Environmental Sciences

_____

by

Alison Renee Sloat

June 2008

CHARACTERIZATION OF NATURAL SPRING WATERS OF THE

SAN BERNARDINO MOUNTAINS USING STABLE

ISOTOPES OF OXYGEN AND HYDROGEN

_____

A Project

Presented to the

Faculty of

California State University,

San Bernardino

_____

by

Alison Renee Sloat

June 2008

Approved by:

23 May 08

Dr. Erik Melchiorre, Chair, Geology   Date

Dr. Brett Stanley, Chemistry

Dr. James Noblet, Chemistry

ABSTRACT

Spring water samples from twenty-five springs in the San Bernardino Mountains of Southern California were collected along the mountain front from 2004 through 2007. Stable isotope measurements of δD and $\delta^{18}O$ were used to identify recharge areas, flow paths, and residence times of hot and cold spring waters. Results for $\delta^{18}O$ range from -4.80 to -8.64‰, and results for δD range from -39.58 to -63.25‰. The results of all stable isotopic analyses, pH, conductivity, water temperature, and flow rates indicate that water recharging the springs in the San Bernardino Mountains originates as recent meteoric precipitation, recent snowmelt runoff, or old geothermal waters. The meteoric waters and snow melt plot on or close to the global meteoric water line. The geothermal waters plot well off of the global meteoric water line, suggesting a source with high temperature and long residence time. Significantly, these geothermal springs appear to have significant circulation depth within the San Andreas Fault System. This bears directly upon understanding which segments of this fault system may be deeply fluid-supported and should assist future seismological studies.

TABLE OF CONTENTS

LIST OF TABLES

LIST OF FIGURES

CHAPTER ONE

INTRODUCTION

Purpose

The purpose of this study was to characterize the natural spring waters of the San Bernardino Mountains using stable isotopes of δD and $\delta^{18}O$.

From October 2004 to December 2007, 85 spring water samples were collected from 25 springs occurring from Devil Canyon to City Creek in the San Bernardino Mountains (Figure 1). Samples from these springs were used to determine stable isotopic temporal and spatial variations, fractionation trends, sources of recharge, and mixing patterns.

The isotopic results of this study will aid with tracing sources, movements, and mixing effects on groundwater receiving mountain-front recharge in the region.

Site Description

The primary area of study includes an approximately 33-square mile (85 km^2) region of the San Bernardino Mountains in Southern California. The northwest-trending San Bernardino Mountains rise from the base of the valley

California State University, San Bernardino
Characterization of Springs of the San Bernardino Mountains
Using Stable Isotopes Study Area Map
Alison Sloat Master's Degree April 2008
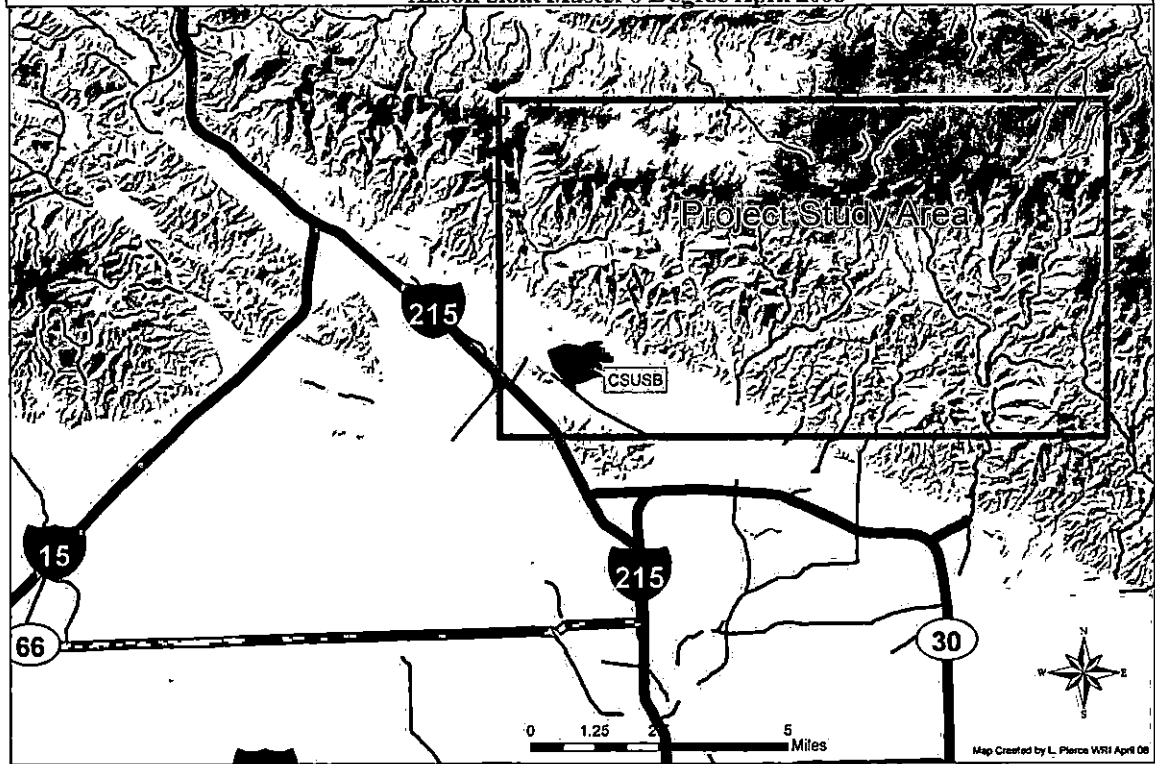
Figure 1. Site Location Map.

floor to over 8,000 feet (2,438m) above mean sea level (amsl) approximately 80 miles (129 km) east of Los Angeles (Figure 2). The study area extends from Devil Canyon east to City Creek, and from the base of the mountains at approximately 1100 feet (335 m) amsl to approximately 2800 feet (853 m) amsl (Figure 3).

Geologic Setting. The San Bernardino Mountains are in the Transverse Range Geologic Province. The San Bernardino Mountains are underlain by Mesozoic granitic and volcanic rocks and by Middle Proterozoic to Pennsylvanian metamorphic rocks. The bedrock consists of Mesozoic granitic rocks and highly metamorphosed Late Proterozoic and Paleozoic metasedimentary rocks deformed by a variety of numerous faults.

The western part of the study area includes a widespread area of the Mesozoic to Proterozoic Gneiss of Devil Canyon which includes schist, layered gneiss, calcsilicate rocks, and marble intruded by Mesozoic monzonite and quartz diorite.

The northwest-trending San Andreas Fault extends through the southwestern study area. The Arrowhead Springs Fault extends from the east to the west of the study area and trends northwest. To the far east, the San Bernardino

3

● Devil Canyon	● Waterman Canyon	● Sand Canyon	Scale 1 : 145728
● Ben Canyon	● Strawberry Creek	● Coldfoot Canyon	
● Badger Canyon	● Borea Canyon	● City Creek	
● Sycamore Canyon	● Little Sand Canyon	—— Study Area Boundary	
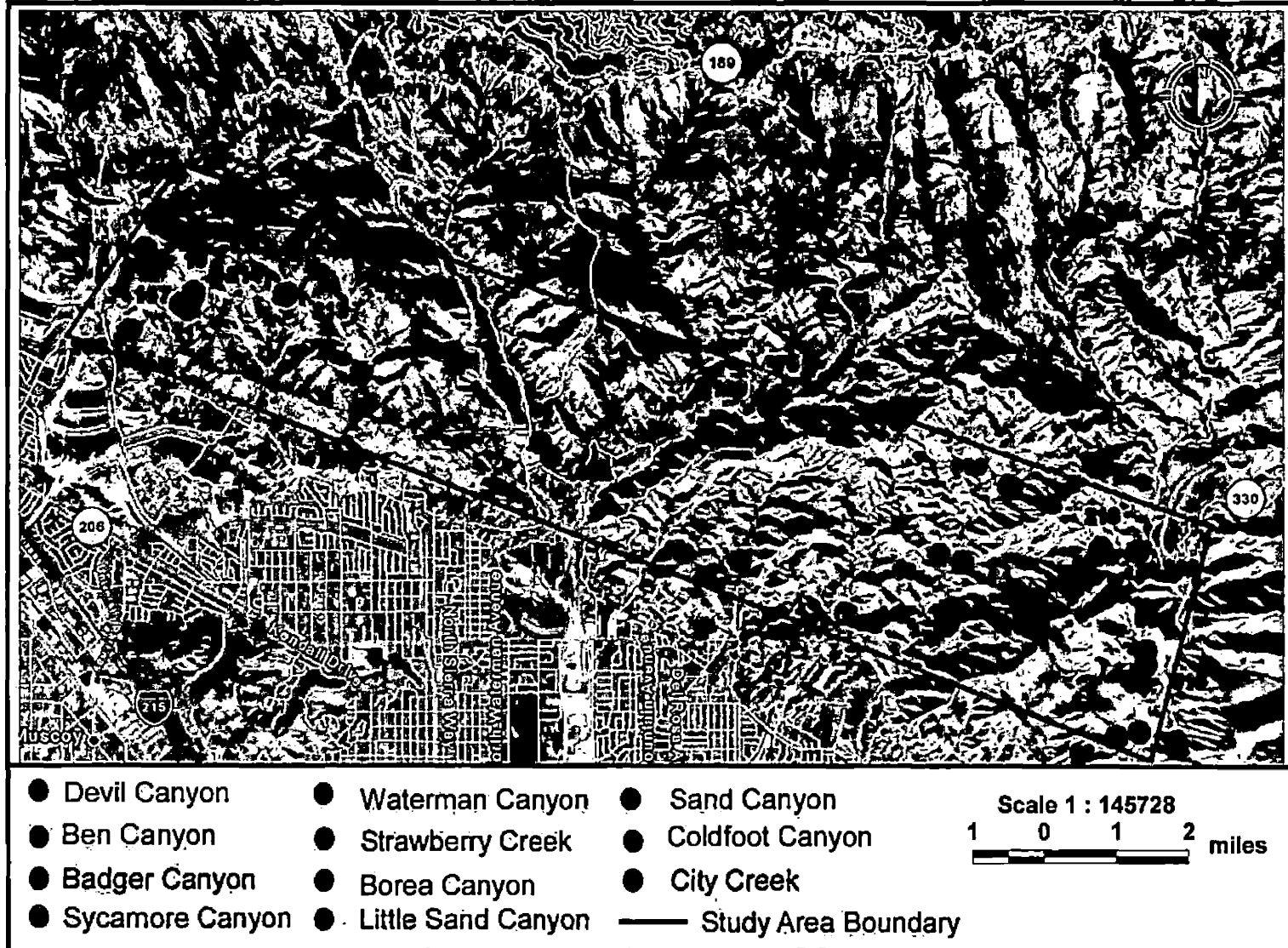
Figure 2: Study Area Sampling Location Map.
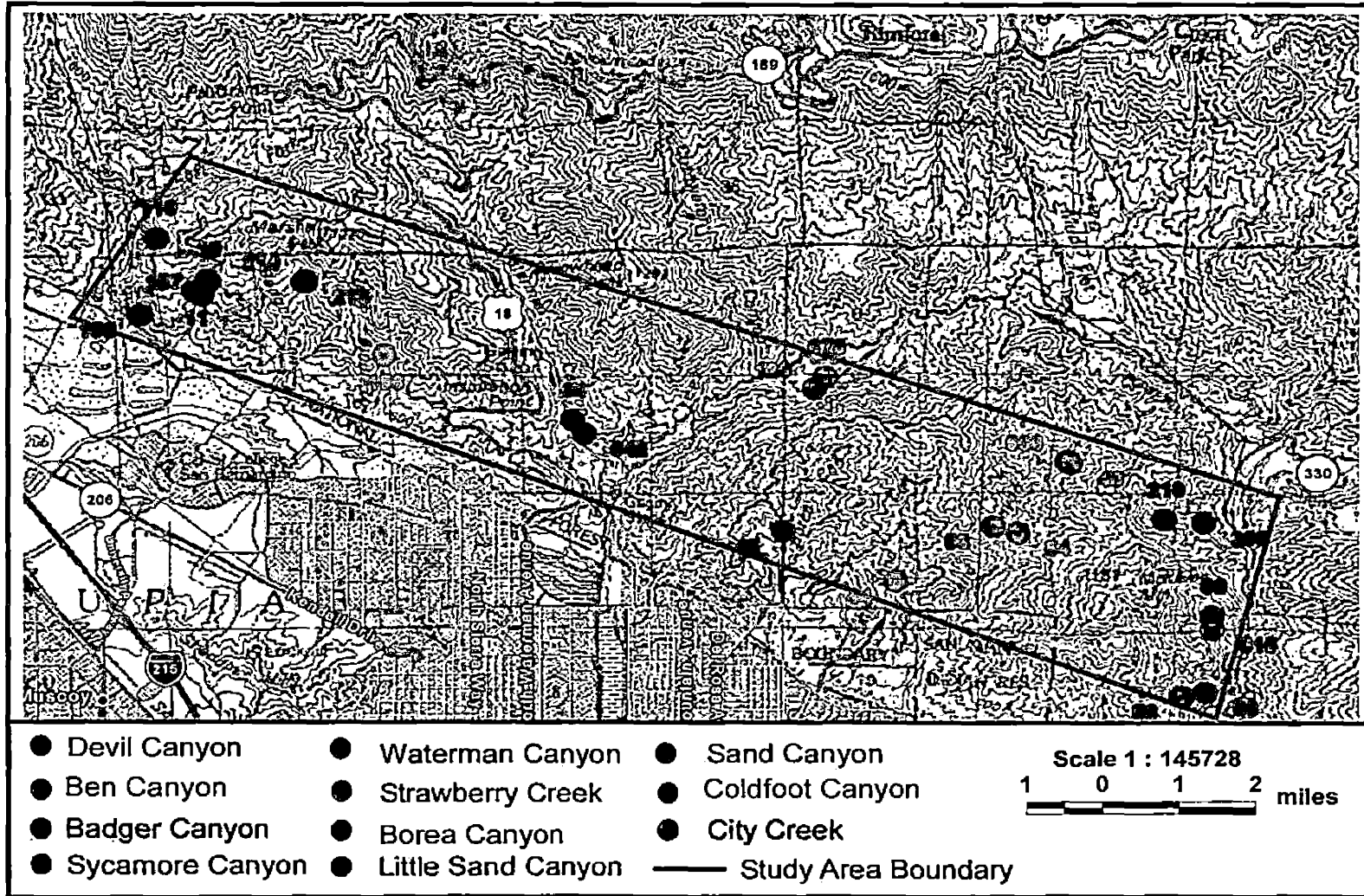
Figure 3: Study Area Topographic Map.

Legend:
- Devil Canyon
- Ben Canyon
- Badger Canyon
- Sycamore Canyon
- Waterman Canyon
- Strawberry Creek
- Borea Canyon
- Little Sand Canyon
- Sand Canyon
- Coldfoot Canyon
- City Creek
- Study Area Boundary

Scale 1 : 145728

1   0   1   2   miles

Mountains are bound by the San Jacinto and San Gorgonio Fault zones (Figure 4).

Springs in the area occur in metamorphic and igneous bedrock including calc-silicate marble, gneiss, quartz monzonite, and granite. Springs in Devil Canyon, Ben Canyon, Badger Canyon, and Sycamore Canyon occur primarily in calc-silicate marble and gneiss. Springs in Waterman Canyon, Strawberry Creek, Borea Canyon, Little Sand Canyon, Sand Canyon, and Coldfoot Canyon occur in quartz monzonite and granite. Springs in City Creek occur in gneiss.

Smaller regional faults include the Ben Canyon Fault, the Badger Canyon Fault, the Sycamore Canyon Fault, the Little Sand Canyon Fault, and the Sand Canyon Fault.

Hydrogeologic Setting. The study area lies within the 120-square mile Bunker Hill Subbasin of the Upper Santa Ana River watershed (Figure 5). Groundwater occurs at depths from approximately 70 feet (21.3 m) below ground surface (bgs) to approximately 420 feet (128 m) bgs (Danskin, 2006).

Annual and perennial streams occur in each canyon in the study area, which is bound to the west by Devil Canyon Creek and by City Creek to the east. The other major stream, Waterman Canyon Creek, is located in the central
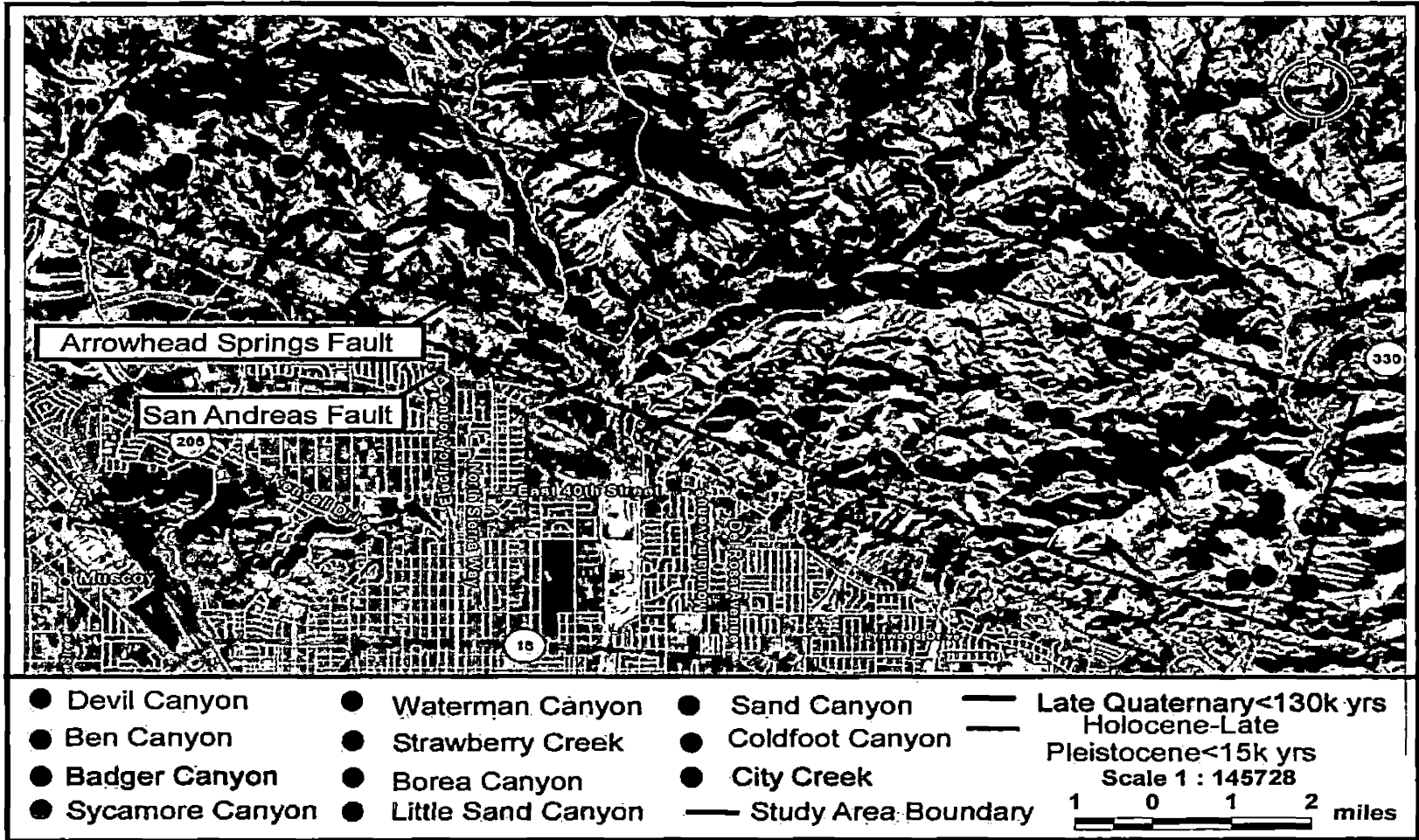
Figure 4: Study Area Fault Location Map.

Legend:
- Devil Canyon
- Ben Canyon
- Badger Canyon
- Sycamore Canyon
- Waterman Canyon
- Strawberry Creek
- Borea Canyon
- Little Sand Canyon
- Sand Canyon
- Coldfoot Canyon
- City Creek
- Study Area Boundary
- Late Quaternary<130k yrs
- Holocene-Late Pleistocene<15k yrs

Scale 1 : 145728

1 0 1 2 miles

Arrowhead Springs Fault

San Andreas Fault
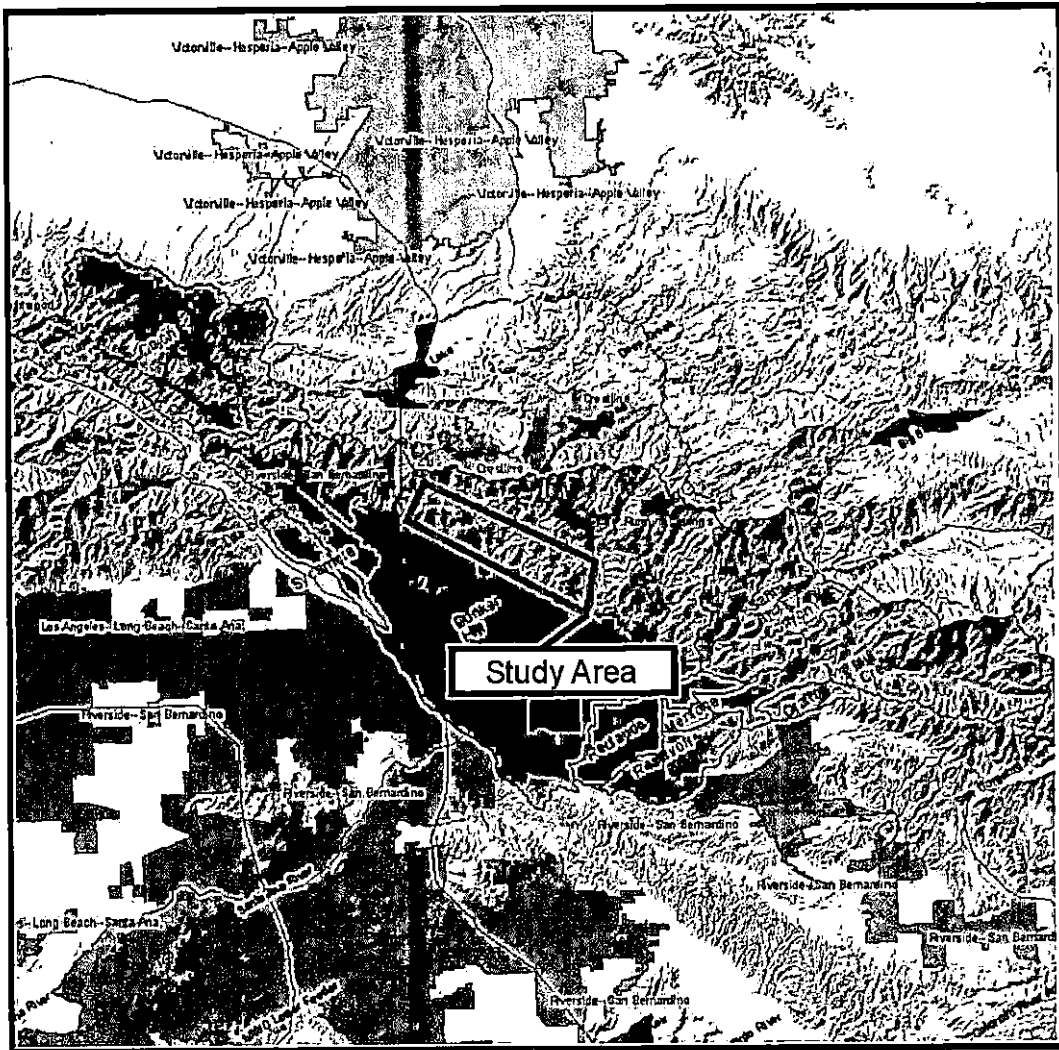
Figure 5. Bunker Hill Subbasin of the Upper Santa Ana River
Watershed.

portion of the study area. Flow from the major streams ranges from 5 gallons per minute (gpm) to 52,000 gpm, depending on the time of year and drought conditions. The average flow rates for Devil Canyon Creek, Waterman Canyon Creek, and City Creek are 1,701 gpm, 1,832 gpm, and 4,244 gpm, respectively. Spring water flows in the study area range from 0.2 gpm to 60 gpm depending on time of year and drought conditions.

Biologic Setting. Springs in the study area provide water for a variety of plants and animals. The study area contains plants typically found in Mediterranean Chaparral Ecosystems. The riparian corridor includes California Black Willow, Mulefat, Virgin's Bower, Black Mustard, Hooker's Evening Primrose, Poison Oak, Tree Tobacco, Mulleins, Cottonwood, Alder, and California Live Oak. Species within the riparian corridor indicative of spring locations, especially during dry summer months include Wild Grape, Yellow Bush Monkeyflower, Watercress, and Mugwort. The mountainous area outside the riparian corridor includes Chamise, Deerweed, Poison Oak, Yerba Santa, Black Mustard, Sycamore, California Black Oak, and California Live Oak.

Climatic Setting. The Mediterranean Southern California climate is characterized by sunny, warm, and dry

weather with winter storms supplying most of the precipitation. Air temperatures range from 35°F (1.67°C) during winter months to over 100°F (37.78°C) during summer months. Rainfall averages from 15 inches per year (in/yr) (38.1 cm/yr) to over 30 in/yr (76.2 cm/yr) depending on location on the mountain front (Danskin, 2006). Storms typically move from the west to the east, with the majority of the precipitation falling in the form of rain at elevations below 6,000 feet (1,829 m), and in the form of snow above 6,000 feet (1,829m).

CHAPTER TWO

STABLE ISOTOPES

Characteristics of Stable Isotopes

Isotopes are atoms of the same element that have nuclei with the same number of protons and electrons but different numbers of neutrons. While an element is defined by its number of protons (Z), an isotope is defined by the number of neutrons (N). For a given isotope ^m_nE, E is the element, m is the mass number, and n is the atomic number of the isotope. The $^{18}_8O$ isotope contains 10 neutrons and 8 protons. There are approximately 300 stable isotopes and 1200 unstable, or radioactive, isotopes (Clark and Fritz, 1997). The greatest stability occurs when the number of neutrons and protons are nearly equal. These stable isotopes lose their stability as the neutron/proton ratio exceeds 1.5. After reaching this point, these isotopes are considered unstable or radioactive.

Isotopes are measured as the ratio of the two most abundant isotopes of a given element. For oxygen, the ratio of ^{18}O with an abundance of 0.204% is compared to ^{16}O, with an abundance of 99.796%. The $^{18}O/^{16}O$ ratio, or the percent natural abundance, is then calculated to be 0.00204. For

hydrogen, the ^{2}H isotope, also denoted D for deuterium, has

an abundance of approximately 0.0156%, while the ^{1}H isotope

has an abundance of about 99.9844%. Hydrogen has a

naturally occurring radioactive isotope, ^{3}H, also known as

tritium. The ^{3}H isotope decays to ^{3}He with a half-life of

12.5 years (Faure, 1986).

These differing isotopic masses cause physiochemical

property differences among isotopes. The structure of the

nucleus dictates physical behavior, whereas the electron

configuration determines the chemical behavior of the

element. The addition or subtraction of one neutron changes

physiochemical properties of elements. For molecules with

different isotopic masses, the heavier isotope has a

stronger bond which requires greater energy to break

compared to the lighter isotope. As a result, lighter

isotopes react more quickly.

The standard to which light stable isotopes are

measured and reported is either Standard Mean Ocean Water

(Craig, 1961), or the equivalent international standard,

Vienna Standard Mean Ocean Water (VSMOW). The difference

between the measured ratios and referenced ratios is

expressed as the delta (δ) notation in parts per thousand

or permil (‰), and is calculated by the following equation:

$$\delta^{18}O_{sample} = \left(\frac{(^{18}O/^{16}O)_{sample}}{(^{18}O/^{16}O)_{reference}} -1 \right) \times 1000‰VSMOW \qquad (Eq.\ 1)$$

The δ values of each standard have been defined as 0‰. A positive δ value signifies that the sample has more ^{18}O than the reference value, or that it is enriched with ^{18}O. A negative δ value signifies that the sample is depleted in the heavier isotope relative to the standard.

Isotope Fractionation

The stable environmental isotopes of hydrogen and oxygen are commonly used in hydrologic investigations to provide information about processes which influence their distribution in the hydrosphere. During fractionation processes, waters and solutes develop isotopic compositions unique to their source or process that formed them. Physical, chemical, and biological processes "fractionate" or change the relative proportions of isotopes through equilibrium and kinetic processes.

Isotope Exchange Reactions. Isotope fractionation or partitioning between two phases occurs through equilibrium isotope exchange reactions. In this process, isotopes of an element are redistributed. At equilibrium, the reaction rates are identical, and the ratios of isotopes are

13

constant for a particular temperature. These processes depend upon the reaction rate differences between molecules. Vibration frequency differences between atoms in molecules of different mass cause preferential isotope fractionation during exchange reactions. Chemical bonds betweens atoms of different isotopic species in molecules with the same chemical formula are sensitive to vibration frequencies, which depend on discrete energy levels of the molecules. Molecules of heavy isotopes are restricted to lower energy levels compared to molecules of light isotopes. Because of this, bonds between light isotopes are weaker than bonds of heavy isotopes. During chemical reactions, lighter isotopes react more readily than those with heavy isotopes.

Partitioning coefficients are produced by the sensitivity of chemical bonds to vibration frequencies between atoms in different molecules. Isotope exchange reactions have partition coefficients that change as temperature is varied. Isotope reactions at high temperatures produce fractionations that change sign and increase in magnitude, and return to zero at very high temperatures (Hoefs, 1987). This "crossover" effect is due to isotope effects which are dependent on the complex

14

nature of thermal excitation of vibration of atoms. Hoefs (1987) defined the partition coefficient as

$$Q = S_i (g_i{}^{(-E_i/KT)})$$ (Eq. 2)

where Q is the partition coefficient, S_i is the statistical weight factor, E_i is the energy level, g_i is the degeneracy or statistical weight of the i_{th} level of E_i, K is the Boltzmann constant, and T is the temperature.

Enrichment of lighter isotopes in the reaction products occurs during non equilibrium chemical reactions. Kinetic isotope effects cause deviations from simple equilibrium processes and are due to the different rates of reaction for various isotopic components that have different atomic masses.

Water-Water Equilibrium Effects. A mass dependent difference in vapor pressure exists between H_2O and HDO and between $H_2{}^{16}O$ and $H_2{}^{18}O$ which causes the hydrogen isotopes to be fractionated in proportion to the oxygen isotopes during all water evaporation and condensation processes. Under equilibrium conditions, H and ^{16}O are partitioned into water vapor during evaporation because $H_2{}^{16}O$ has a higher vapor pressure than HDO and $H_2{}^{18}O$. Precipitation follows a

15

Rayleigh process at liquid-vapor equilibrium, and the liquid phase is enriched in D and ^{18}O because $H_2^{18}O$ has a lower vapor pressure than H_2O and $H_2^{16}O$. The actual isotopic composition of water vapor is lighter and precipitation heavier than the predicted equilibrium values because of kinetic effects (Hoefs, 1987, Dansgaard, 1964).

Water-Water Kinetic Effects. Kinetic effects, or non equilibrium processes, are suggested as the consequence of different reaction rates of various isotopic components (Dansgaard, 1964). Kinetic effects are dependent on molecular weights, bond strengths, and diffusion rates. Bonds between molecules in light isotopes are weaker than bonds in heavier isotopes, causing molecules with lighter isotopes to react more readiy than those with heavy isotopes during chemical reactions. Because of this, the molecules with lighter isotopes are preferentially partitioned into the reaction product during non equilibrium chemical reactions.

Light isotopes are generally more mobile than heavy isotopes. Dansgaard (1964) showed that extremely fast evaporation causes the deuterium component to be much less sensitive to kinetic effects than the ^{18}O component. In water vapor, the light isotope of water H_2O^{16} reacts or

evaporates faster than the heavier ^{18}O because the isotopic components have different rates of reaction, as shown in Equation 3:

$$c(H_2O^{16}) > c(HDO^{16}) > c(H_2O^{18}) \qquad (Eq. 3)$$

where c is the rate of reaction. Other variables, such as temperature, wind speed, and water turbulence add to the complexities of kinetic effects.

Use of Stable Isotopes in Hydrology

Hydrogen and oxygen isotopes in hydrological investigations are useful for tracing waters and providing information on type, origin, and age of waters (Kendall, 1998). The variation of oxygen isotopes is expressed as enrichment (a more positive value) or depletion (a more negative value) of the less abundant isotope, ^{18}O, with respect to the more abundant ^{16}O. Similarly, the isotopic variation of hydrogen is expressed as enrichment or depletion of the less abundant isotope, ^{2}H, with respect to the more abundant ^{1}H relative to SMOW.

The largest reservoir of water in the hydrosphere, the ocean, has been found to be relatively homogeneous with

respect to hydrogen and oxygen composition. Ocean water was set as a standard by Craig (1961) for relating measurements of ^{18}O and D. Although the average isotopic composition of the Earth's oceans remains constant, small regional deviations occur because of surface evaporation and glacial melting, which constantly enrich the upper layers with heavy isotopes. An isotopic water balance between ocean water, evaporation, condensation, runoff, and ocean water mixing maintains a constant isotopic composition of the ocean.

Fractionation Mechanisms in the Water Cycle

Each segment of the atmospheric evaporation-precipitation cycle acts like a distillation column or Rayleigh fractionation process, where a phase change removes water from a relatively homogeneous reservoir (Epstein and Mayeda, 1953; Dansgaard, 1964). Evaporation dominates because of high temperatures at low latitudes, favoring the lighter isotope in the vapor phase. Precipitation dominates at high latitudes. During rain events, the light ^{1}H and ^{16}O remain in the vapor phase while the heavier isotopes rain out, depleting the north and south latitudes with heavier isotopes in the vapor phase.

This "latitude effect" over North America is approximately 0.5‰ $\delta^{18}O$ per degree latitude (Dansgaard, 1964, Gat, 1980). Over marine areas, precipitation at any given latitude is more ^{18}O-rich than continental precipitation, and reflects about a 0.044‰ $\delta^{18}O$ per degree north or south latitude effect. As warm surface water currents such as the North Atlantic Drift move from the Gulf of Mexico to the Caribbean Sea, continuous evaporation and rainout effects without elevation effects keep isotopic signatures constant. Continental effects occur as topography and temperature extremes cause the rain out of heavier isotopes near coastal regions and depleted isotopes in the inner continental areas (Dansgaard, 1964).

Variations in the worldwide meteoric water, derived from precipitation and surface water samples by Craig (1961), represent the relative proportion of hydrogen and oxygen isotope variations:

$$\delta D = 8 \; \delta^{18}O + 10 \qquad \qquad \text{(Eq. 4)}$$

where 8 is the slope of the "meteoric water line", and 10 is the deuterium excess. A plot of δD versus $\delta^{18}O$ represents this "meteoric water line" (MWL), which varies locally

depending on evaporation, condensation, and vapor phase
transport characteristics which affect the deuterium excess
(Dansgaard, 1964).

The MWL is relatively constant for precipitation
worldwide, although small variations may occur as a result
of closed or partially closed hydrologic systems. Varying
temperatures, climatic conditions, precipitation, winds,
humidity, and topography can all affect the signature of
isotopes in a system.

The MWL represents a linear interdependence of H- and
O-isotope ratios for meteoric waters that have not
undergone significant evaporation. The slope of the MWL
represents the ratio of δD and $\delta^{18}O$ fractionation factors at
the condensation temperatures. Because this ratio is
relatively constant for worldwide precipitation, worldwide
precipitation events plot consistently along the MWL
because of the common $\delta D/\delta^{18}O$ ratio over certain ranges of
condensation temperatures. Evaporation and small changes in
temperature cause small variations from the MWL.

Craig (1961) conducted laboratory evaporation studies
exhibiting that at earth surface temperatures, heavy
isotope enrichment consistently follows a slope of about
five. Mixing from precipitation events along with recharge

from surface water cause evaporative trends with slopes between five and eight occur in open water bodies under natural atmospheric conditions.

Horizontal shifts in the meteoric water line represent decreasing $\delta D / \delta^{18}O$ ratios with increasing high-temperature water-rock isotope exchange in hot spring and geothermal systems. Because oxygen is much more abundant in rocks and minerals compared to hydrogen, preferential ^{18}O exchange occurs from rock to fluid under high temperature conditions, producing a flat slope in the meteoric water line as little deuterium exchange occurs.

Physiographic Isotope Effects

In addition to latitude dependence, climate and topography affect isotope characteristics. Rayleigh fractionation, produced by evaporative and precipitation processes of the water cycle, describes the gross isotope characteristics observed in meteoric surface and groundwaters.

Gat (1980) noted a few problems with the use of a simple Rayleigh fractionation mechanism to describe all isotopic variations in meteoric waters. It was argued that air flow patterns are not simple processes of poleward

21

drift of low-latitude air masses, the meteoric water line

is not predicted to be mathematically straight when

integrating ^{18}O and ^{2}H simultaneously, and the latitudinal

distillation column is not a closed system because of

supplemental evaporation over middle- and high-latitude

oceans.

Geographic features influence the isotopic composition

of precipitation. The Rayleigh fractionation process

depletes the water vapor cloud and the rainfall in the

heavier isotopes of hydrogen and oxygen, producing "rain

out" effects, rain shadow effects, and temperature effects.

The altitude effect, which depends on local climate

and topography, favors the lighter isotopes in the vapor

phase. Low elevation precipitation is usually enriched in

heavy isotopes as the heavy isotopes "rain out" at the

lower elevations. Isotopically heavy precipitation is

forced from inland-migrating storms at lower elevations of

mountain fronts, leaving the lighter ^{16}O and ^{1}H in water

vapor to precipitate at higher elevations. Gradients of

0.15 − 0.5‰ $\delta^{18}O$ per 100m and 1.2 − 4.0‰ δD per 100m are

characteristic of the northern hemisphere (Gat, 1980).

The distance inland, or "rain-out" effect, implies

depletion of ^{18}O and ^{2}H as rain or snow is progressively

22

released from clouds as storm systems move up and over topographic highs. Inland-advancing clouds initially evaporated from marine waters become isotopically depleted with continued precipitation and movement from the marine source, over the topographic high, and in to lower continental areas. δD depletion trends of western North America regions range from -0.2‰ per 100km to -60‰ per 100km in elevation gain (Ingraham, 1988).

The rain shadow effect occurs on the leeward side of mountains as the heavier isotopes rain out. As the precipitation becomes more depleted as it moves up and over the mountainous regions, less water is available to precipitate in the rain shadow areas. This explains why mountainous regions receive a large amount of isotopically depleted precipitation, while adjacent topographic saddles and desert regions receive small amounts of depleted precipitation.

CHAPTER THREE

PREVIOUS WORK

Isotope Hydrology

Isotope investigations focusing on isotopic

differences between fresh and ocean waters were conducted

by Epstein and Mayeda (1953) and Friedman (1953). Dansgaard

(1953, 1954, and 1964) and Epstein (1956) focused on

isotopic compositions of precipitation. Equilibrium and

kinetic isotope exchange effects were initially conducted

by Friedman et al. (1962). Craig (1961) also focused on the

evaporative isotope effects in lakes and other water bodies

worldwide. Ingraham and Taylor (1986, 1991) studied

climatic and isotopic processes related to inland-

precipitating climatic systems.

Studies conducted by Friedman et al. (1964) focusing

on physiographic isotope effects and inland effects on

surface waters in North America were followed by studies

conducted by Friedman and Smith (1970 and 1972) that showed

orographic effects across the Sierra Nevada. Williams and

Rodoni (1992, 1993) focused on investigations using stable

isotopes in southern California hydrogeological studies.

Isotopic compositions of groundwaters in southeastern

California were presented for Orange County, the Inland Empire, and the State Water Project by Rodoni (1993). The values presented for San Bernardino Mountain groundwaters exhibited orographic and rain-out trends and ranged in composition from -13 to -8‰ for $\delta^{18}O$, while the values for δD ranged from -90 to -45‰. Smith et al. (1992) and Friedman et al. (1992) presented depleted isotopic values for precipitation and groundwater in southeastern California indicating recharge sources from older Pleistocene waters rather than modern snow and precipitation sources.

Studies conducted near the Newmark Area of San Bernardino by Izbicki et al. (1998) showed that $\delta^{18}O$ and δD isotopic compostions of groundwaters from wells ranged from -7.7 to -8.3‰ and -49 to -53‰. Waters plotting above the local meteoric water line were assumed to be snowmelt runoff, as a result of orographic and evaporation effects with increasing altitude causing depletion of water vapor and precipitation (Magaritz et al., 1989).

Isotopic values presented by Rose et al. (1996) for springs in a fractured system in northeastern California showed that orographic effects cause the depletion of spring water isotopic values as elevation increases at the

rate of approximately -0.71‰ per 1000 feet of elevation
gain. Isotopic values for low conductivity springs near the
same area showed a decrease in isotopic values at the rate
of approximately 0.68‰ per 1000 feet of elevation gain
(Melchiorre et al., 1999). Increases in co- and post-
seismic groundwater discharge at the surface through a
spring, seep, or stream was also shown to be caused by an
increase in vent or fracture conductance within the fault
system (Muir-Wood and King, 1993).

White et al. (1973) showed the relationship between
isotopic values of non-meteoric waters in geothermal
systems, as geothermal waters continuously plot below the
MWL. Clark and Fritz (1997) showed the range of isotopic
values typical for waters found in water-rock interaction
systems. The values for oxygen isotopes in meteoric,
geothermal, seawater, magmatic, and metamorphic systems
were presented along with hydrogen isotopic values found in
basaltic, granitic, and metamorphic rock systems. Fournier
and Thompson (1980) used isotopes to demonstrate slow
recharge movement and a large rock-to-water $\delta^{18}O$ ratio in
thermal springs with Sierra Nevadan recharge in the Coso
Range.

Studies conducted by Abbott et al. (2000), Mayr et al (2007), and Paternoster et al. (2007) focused on the use of stable isotopes to interpret recharge patterns in bedrock aquifers. Seasonal isotopic variations in groundwater and precipitation values were used to track patterns within watershed hydrologic systems. Nathenson et al. (2003) used stable isotopes to study recharge elevations at slightly thermal and non-thermal springs at Mt. Shasta. Isotopic values at spring locations at lower elevations indicated longer flow paths with meteoric sources, while isotopic values at higher elevations indicated shorter flow paths of geothermal sources for spring waters. Isotopes have also been used as tools in studying recharge at the mountain-front (Blasch and Bryson, 2007). Isotopic values from precipitation events along the mountain-front were compared to values in basin wells to determine the location where precipitation entered the local groundwater system.

CHAPTER FOUR

METHODS

Sample Collection

Samples from 25 springs in the San Bernardino Mountains were collected from October 2004 through December 2007 (Table 1). Eighty-five (85) samples were collected in the late fall, mid-winter, and early spring to determine isotopic composition, seasonal $\delta^{18}O$ and δD variations, and sources of recharge within the regional groundwater system. Samples were collected before the first rain storms in the fall. Samples collected in mid-winter and early spring were collected at least two weeks after rain events. Samples were collected in 25mL glass jars with poly-lined lids, labeled, and stored until analysis.

Measurements of pH, conductivity, water temperature, and air temperature were measured in the field at the time of collection using a portable Hanna Instruments combination pH/conductivity/temperature probe. Calibration of the field instrument was conducted each day before sample collection. Spring discharge rates were measured volumetrically with a bucket.

Table 1. Site Locations

Site	Canyon	Latitude	Longitude	Elevation (feet)
9	Ben	34.203734000000	-117.32102000000	2305.6
10	Ben	34.205435000000	-117.31979600000	2419
11	Ben	34.204808000000	-117.32004200000	2364.1
44	Little Sand	34.168498000000	-117.22874600000	1872.5
45	Borea	34.174625000000	-117.24358200000	1857
48	Sand	34.183046000000	-117.20597500000	2534.3
53	Sand	34.175332000000	-117.21588700000	2087.1
54	Sand	34.174534000000	-117.21255300000	2086.6
56	City Creek	34.154442000000	-117.19102400000	2115.3
58	City Creek	34.154832000000	-117.18761300000	1917.4
59	City Creek	34.164305000000	-117.18725800000	2283.2
94	Waterman	34.188064000000	-117.27096100000	1923.2
110	Devil	34.210363000000	-117.32603000000	2436.5
120	Strawberry	34.192249000000	-117.23952900000	2193.5
153	Ben	34.205091000000	-117.32929800000	2004.2
156	Sycamore	34.196342000000	-117.29685000000	2116.2
157	Ben	34.204544000000	-117.32018500000	2511.9
209	Coldfoot	34.175781000000	-117.18837100000	2336.7
210	Coldfoot	34.176171000000	-117.19378000000	2574.9
213	Badger	34.205165000000	-117.30641000000	2720
214	Badger	34.205259000000	-117.30705200000	2712.2
515	City Creek	34.162708000000	-117.18710500000	2230.5
636	Sand	34.183299000000	-117.20627800000	2560
642	Waterman	34.186942000000	-117.27058600000	1923.2
678	Strawberry	34.193626000000	-117.23821300000	2203

Sample Analyses

Sample analyses were conducted at the University of California Davis Stable Isotope Facility using a Los Gatos Research DLT-100 Laser Absorption Spectroscopy Isotope Ratio Mass Spectrometer. Before shipment to Davis, 1mL samples were transferred into labeled 2mL standard gas chromatography vials. Samples were injected six times each, with the first three injections discarded to avoid "memory." The average of injections four through six were used for isotope ratio calculations, with VSMOW used as the reference standard. The precision was recorded as <0.3‰ for $\delta^{18}O$ and <0.8‰ for δD (Table 2).

Table 2. Sampling Data Results

Site	Canyon	Sampling Date	Elev (ft)	pH	EC (µS/cm)	Water Temp (°F)	Air Temp (°F)	Flow (gpm)	δD (‰)	δ^{18}O (‰)	Predict MWL
110	Devil	10/13/2006	2437	8.70	513	59	65	0.8	−49.87	−7.93	−53.44
110	Devil	1/30/2007	2437	8.60	560	49	60	2.5	−50.39	−7.98	−53.84
110	Devil	3/22/2007	2437	6.90	538	59	65	1.9	−49.97	−7.67	−51.33
9	Ben	10/7/2004	2305	8.60	840	63	63	0.3	−51.10	−7.88	−53.04
9	Ben	11/5/2004	2305	8.30	1050	58	56	2.7	−49.00	−7.52	−50.16
9	Ben	1/23/2007	2305	8.50	587	56	50	7.5	−49.54	−7.75	−52.03
9	Ben	12/11/2007	2305	7.80	601	54	47	4.5	−50.49	−7.91	−53.31
10	Ben	11/5/2004	2419	8.50	730	53	55	0.8	−47.90	−7.33	−48.64
10	Ben	1/23/2007	2419	8.30	499	55	60	2.5	−51.54	−7.93	−53.44
10	Ben	12/11/2007	2419	7.70	557	56	55	2.2	−51.09	−7.87	−52.98
11	Ben	11/7/2004	2364	9.10	550	60	48	0.3	−50.40	−7.66	−51.28
11	Ben	10/6/2006	2364	8.80	537	58	60	3.0	−51.02	−7.79	−52.30
11	Ben	1/23/2007	2364	8.80	512	56	65	0.8	−49.27	−7.51	−50.06
11	Ben	3/22/2007	2364	7.00	535	70	80	1.0	−50.25	−7.64	−51.12
11	Ben	12/11/2007	2364	8.00	524	54	60	1.5	−51.57	−7.69	−51.52
153	Ben	10/6/2006	2004	7.70	678	67	60	0.1	−48.62	−7.48	−49.81
157	Ben	11/5/2004	2511	8.60	640	51	55	0.1	−49.70	−7.62	−50.96
157	Ben	10/6/2006	2511	8.10	515	60	60	0.5	−39.58	−4.80	−28.44
157	Ben	1/23/2007	2511	8.50	523	52	60	0.4	−50.99	−7.88	−53.03
157	Ben	3/22/2007	2511	6.90	526	58	73	0.1	−45.36	−6.51	−42.05
157	Ben	12/11/2007	2511	7.81	478	53	49	0.3	−49.39	−8.06	−54.46
213	Badger	9/24/2004	2720	8.90	580	56	64	0.6	−51.10	−7.83	−52.64
213	Badger	10/20/2006	2720	8.60	543	67	65	1.9	−52.79	−8.17	−55.37
213	Badger	1/11/2007	2720	8.70	506	51	52	1.5	−52.19	−8.12	−54.92
213	Badger	12/11/2007	2720	7.60	521	48	44	2.2	−52.56	−8.13	−55.04
214	Badger	9/24/2004	2720	8.60	540	56	64	0.1	−50.10	−7.68	−51.44
214	Badger	10/20/2006	2712	8.60	498	57	65	2.5	−51.62	−8.19	−55.54
214	Badger	1/11/2007	2712	8.50	475	48	52	2.5	−51.61	−8.31	−56.48
214	Badger	12/11/2007	2712	7.90	473	46	44	3.5	−51.89	−8.10	−54.82

Table 2. Sampling Data Results

Site	Canyon	Sampling Date	Elev (ft)	pH	EC (µS/cm)	Water Temp (°F)	Air Temp (°F)	Flow (gpm)	δD (‰)	$\delta^{18}O$ (‰)	Predict MWL
156	Sycamore	10/4/2006	2116	8.20	442	62	65	1.1	−52.72	−8.09	−54.74
156	Sycamore	1/23/2007	2116	8.60	458	45	57	0.5	−53.02	−8.06	−54.52
94	Waterman	10/11/2004	1954	9.20	1660	190	68	48.0	−63.01	−8.64	−59.09
94	Waterman	10/13/2006	1954	8.70	1492	182	72	42.5	−63.25	−8.54	−58.30
94	Waterman	1/19/2007	1954	9.00	1430	184	65	50.0	−61.04	−8.39	−57.09
94	Waterman	3/12/2007	1954	8.50	1552	186	63	50.0	−61.27	−8.57	−58.56
94	Waterman	12/10/2007	1954	8.06	1337	192	64	60.0	−61.78	−8.60	−58.77
642	Waterman	10/13/2006	1922	8.10	1411	90	68	2.2	−59.21	−8.51	−58.08
642	Waterman	12/10/2007	1922	7.84	1295	88	64	1.9	−60.03	−8.42	−57.36
120	Strawberry	10/12/2004	2345	8.20	250	64	73	1.9	−51.70	−7.52	−50.16
120	Strawberry	2/15/2007	2345	7.90	332	50	67	0.3	−50.45	−7.86	−52.87
678	Strawberry	10/12/2006	2387	8.50	298	59	72	0.2	−50.61	−7.70	−51.61
678	Strawberry	2/15/2007	2387	8.10	324	52	64	0.2	−50.10	−7.65	−51.20
678	Strawberry	3/15/2007	2387	8.40	314	64	78	0.1	−49.37	−7.62	−50.96
45	Borea	9/27/2004	1858	8.60	360	66	65	7.2	−51.50	−7.79	−52.32
45	Borea	11/8/2004	1858	8.50	370	67	58	6.6	−50.70	−7.62	−50.96
45	Borea	10/16/2006	1858	8.20	358	66	62	6.0	−50.78	−7.68	−51.45
45	Borea	1/29/2007	1858	8.40	369	65	65	5.5	−50.16	−7.56	−50.46
45	Borea	3/16/2007	1858	8.10	353	71	82	4.3	−51.87	−7.60	−50.78
44	Little Sand	10/6/2004	1873	8.90	310	68	62	4.0	−51.30	−7.66	−51.28
44	Little Sand	11/4/2004	1873	8.60	290	64	58	4.4	−51.60	−7.65	−51.20
44	Little Sand	10/9/2006	1873	8.30	286	67	61	7.5	−50.45	−7.63	−51.03
44	Little Sand	1/29/2007	1873	8.30	288	63	59	6.0	−51.45	−7.83	−52.67
44	Little Sand	3/16/2007	1873	8.20	298	68	70	5.5	−55.18	−7.81	−52.46
48	Sand	11/16/2004	2534	8.80	440	58	55	3.2	−54.10	−8.20	−55.60
48	Sand	10/11/2006	2534	8.90	401	57	57	5.0	−53.43	−8.12	−54.97
48	Sand	2/7/2007	2534	9.00	388	54	62	5.5	−52.92	−8.35	−56.82
48	Sand	3/14/2007	2534	8.60	403	54	55	3.0	−52.99	−8.39	−57.16
48	Sand	12/12/2007	2534	7.80	477	44	44	18.0	−52.84	−8.23	−55.88

Table 2. Sampling Data Results

Site	Canyon	Sampling Date	Elev (ft)	pH	EC (µS/cm)	Water Temp (°F)	Air Temp (°F)	Flow (gpm)	δD (‰)	$\delta^{18}O$ (‰)	Predict MWL
53	Sand	10/11/2006	2087	8.50	378	57	63	1.5	-51.12	-7.65	-51.19
53	Sand	2/7/2007	2087	8.60	368	50	70	1.5	-52.20	-7.80	-52.37
53	Sand	3/14/2007	2087	8.30	396	58	70	0.9	-49.83	-7.20	-47.58
53	Sand	12/12/2007	2087	7.70	451	46	44	1.5	-52.59	-8.21	-55.68
54	Sand	10/11/2006	2087	8.20	351	55	56	7.5	-50.69	-8.12	-54.93
54	Sand	2/7/2007	2087	8.20	327	50	67	7.0	-50.22	-8.03	-54.25
54	Sand	3/14/2007	2087	7.80	339	55	66	5.5	-50.24	-7.59	-50.73
54	Sand	12/12/2007	2087	7.70	359	44	39	7.0	-52.51	-7.95	-53.60
636	Sand	10/11/2006	2560	8.50	500	55	52	6.0	-47.81	-6.92	-45.38
636	Sand	2/7/2007	2560	8.80	494	49	64	9.0	-43.97	-6.65	-43.22
636	Sand	3/14/2007	2560	8.40	518	54	62	9.0	-47.50	-7.16	-47.26
209	Coldfoot	10/12/2006	2337	8.60	404	55	64	1.1	-47.00	-7.79	-52.34
209	Coldfoot	2/9/2007	2337	8.90	382	46	62	2.5	-48.72	-7.47	-49.73
209	Coldfoot	12/12/2007	2337	7.70	427	42	49	2.2	-51.77	-7.81	-52.50
210	Coldfoot	10/12/2006	2575	9.10	306	62	66	0.5	-50.28	-7.27	-48.18
210	Coldfoot	2/9/2007	2575	8.70	318	50	67	0.6	-50.42	-8.02	-54.12
210	Coldfoot	12/12/2007	2575	7.80	302	45	55	1.5	-50.36	-7.42	-49.39
56	City Creek	11/4/2004	2115	8.70	910	57	64	0.6	-53.40	-7.82	-52.56
56	City Creek	1/26/2007	2115	8.50	722	57	68	2.5	-52.74	-7.81	-52.44
58	City Creek	10/1/2004	1917	9.20	530	60	67	0.0	-51.90	-7.56	-50.48
58	City Creek	11/4/2004	1917	9.00	1090	57	65	0.2	-47.30	-6.75	-44.00
59	City Creek	10/12/2006	2283	8.40	615	58	59	0.3	-49.47	-7.48	-49.80
59	City Creek	2/15/2007	2283	8.30	610	53	64	0.6	-49.58	-7.44	-49.56
59	City Creek	3/15/2007	2283	7.90	582	61	81	0.4	-48.94	-7.38	-49.07
515	City Creek	10/12/2006	2231	8.20	493	57	60	0.8	-51.18	-8.12	-54.94
515	City Creek	2/15/2007	2231	8.10	480	50	62	1.5	-50.34	-7.78	-52.26
515	City Creek	3/15/2007	2231	8.00	527	62	76	1.2	-51.45	-7.96	-53.69

CHAPTER FIVE

RESULTS AND DISCUSSION

Results

The results of all stable isotopic analyses, pH, conductivity, water temperature, and flow rates are presented in Table 2.

The isotopic results plot roughly along the meteoric water line (MWL) established by Craig (1961) and are presented in Figure 6. Results for $\delta^{18}O$ range from -4.80 to -8.64‰. Results for δD range from -39.58 to -63.25‰.

The predicted MWL was calculated using Craig's Meteoric Line equation (Equation 4) and the measured values of $\delta^{18}O$ to determine the predicted δD values (Table 2). The predicted δD and measured $\delta^{18}O$ values were plotted to determine the local meteoric line. The local MWL for the study area is not distinguishable as a separate line from Craig's MWL on a δD vs. $\delta^{18}O$ plot. With a few exceptions, the majority of the spring locations plot along the MWL, indicating that the major source of recharge for springs in the study area is meteoric precipitation.

Several springs, including Site 157 in Ben Canyon, and Sites 94 and 642 in Waterman Canyon, deviate from this MWL

line in an evaporative trend, indicating a significant non-meteoric or modified meteoric component (Figure 6). A plot of the spring elevation and $\delta^{18}O$ in Figure 7 shows the isotopic change with elevation. As elevation increases, the isotopic values in the springs become more negative at an average rate of -0.59‰ per 1000 feet of elevation gain (-1.94‰ per 1000m) (Figure 8). This is slightly lower than the average value of -0.71 per 1000 feet from Rose et al. (1996) and Melchiorre et al. (1999). Springs not affected by meteoric recharge do not demonstrate this trend. Figure 7 shows that these non-meteoric recharged springs include Ben Canyon, Waterman Canyon, and Coldfoot Canyon. Springs in these areas are likely recharged by means other than meteoric precipitation, and are not included in Figure 8.

Hot Springs in Waterman Canyon

Sites 94 and 642 in Waterman Canyon occur at the lower elevations in the study area at 1954 feet (596 m) amsl and 1922 feet (586 m) amsl, respectively. Spring water temperatures for Site 94 ranged from 182°F (83.33°C) to 192°F (88.89°C). Spring water temperatures for Site 642 ranged from 88°F (31.11°C) to 90°F (32.22°C) (Table 2). Because water temperatures for these two sites are significantly higher than temperatures in springs in the
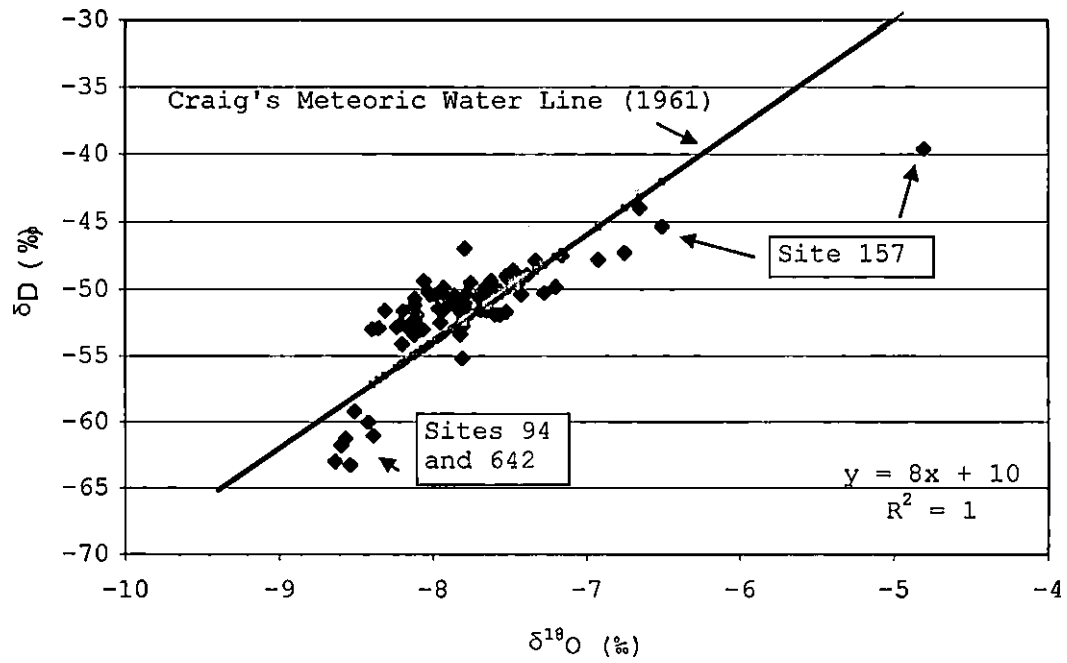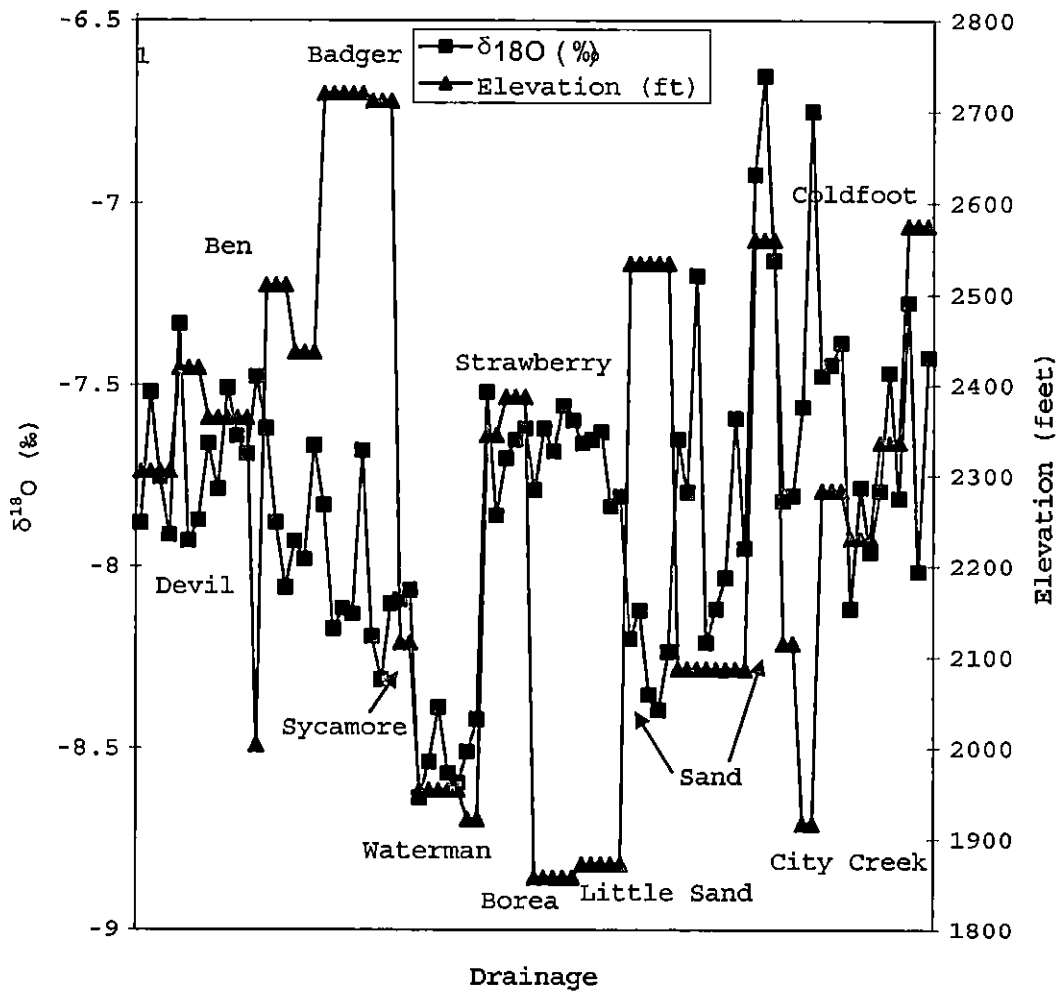
Figure 6. Isotopic Results

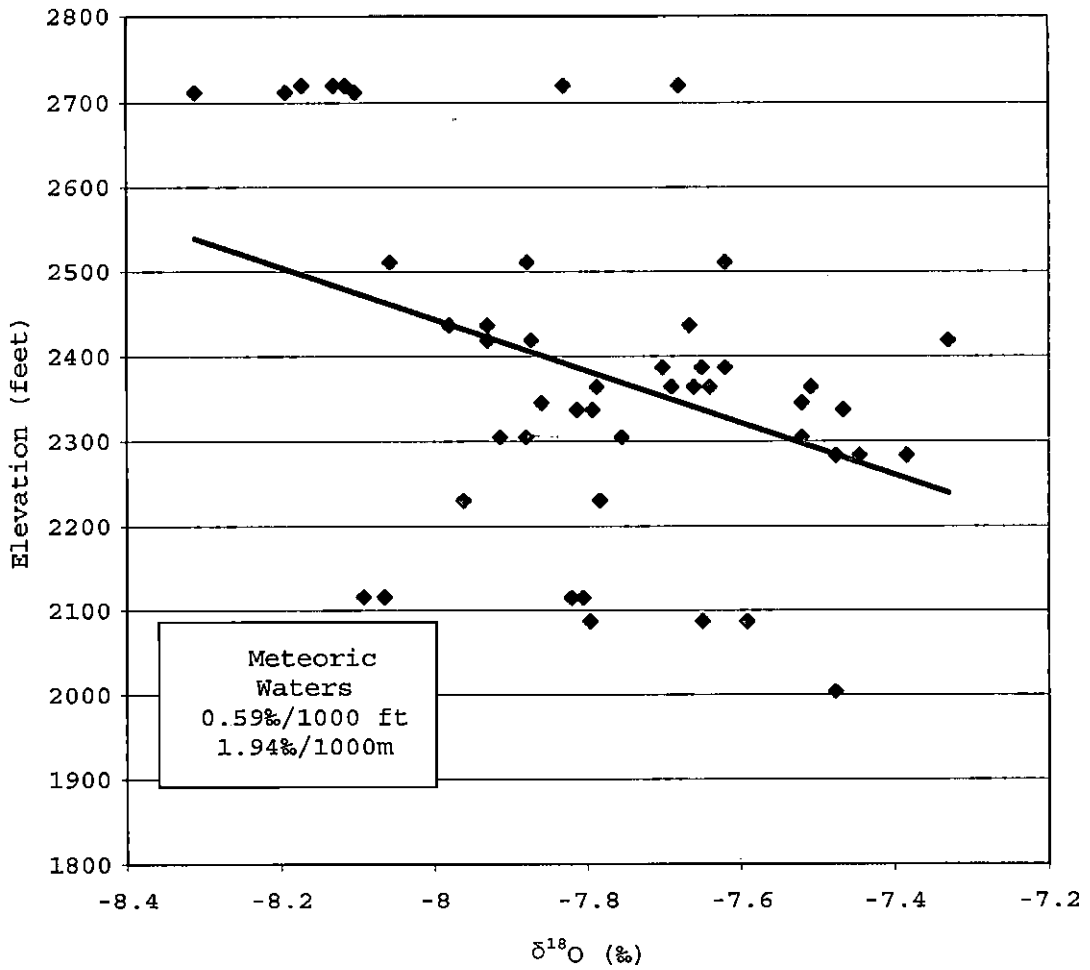Figure 7. Oxygen Isotopic Change With Elevation

Figure 8. Isotopic Change With Elevation

surrounding area, it is almost certain that the source of recharge for these springs occurs within a deeper-circulating water source.

The two spring locations are located between two sections of the Arrowhead Springs Fault (Figure 3). This suggests a possible barrier to groundwater flow and source for deeper groundwater circulation within the fault bounded area.

The range of isotopic values for these two hot springs ($\delta^{18}O$ = -8.6 to -8.3‰, δD = -63.2 to -59.2‰) occurs within the range for waters characteristic of geothermal waters (Clark, 1997). The water samples from Sites 94 and 642 plot to the lower right of the meteoric line (Figure 9). As meteoric water flows into a geothermal system and becomes heated, light meteoric oxygen and hydrogen exchange with heavier oxygen and hydrogen in the surrounding rock. Because rock contains a small amount of hydrogen and a large amount of oxygen, the oxygen isotopic composition of the water changes, while the hydrogen isotopic composition does not. As a result, the magnitude of the $\delta^{18}O$ shift in the water indicates the relative amount of meteoric water that has exchanged with the rock. The δD shift is indicative of the amount of meteoric recharge water.
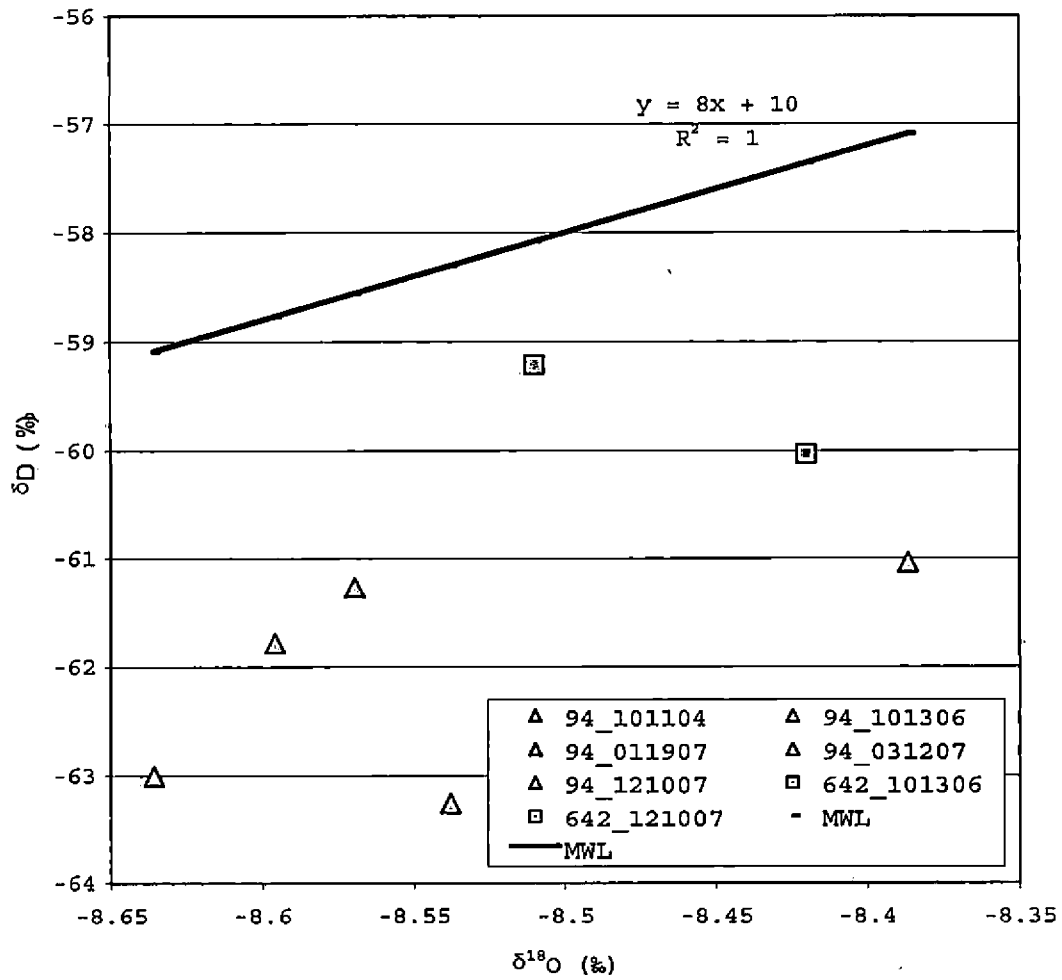
Figure 9. Waterman Canyon Isotopic Results

The $\delta^{18}O$ and δD values for Sites 94 and 642 indicate
that recharge comes from both geothermal and meteoric
water. Mixing calculations show that both springs have
meteoric water influence, with 62% to 86% of meteoric water
contributing to recharge in both springs (Appendix A). The
higher temperature spring at Site 94 exhibits the lower
percentage of meteoric recharge. Because of the constant
high temperature of these springs and the depleted isotopic
values, the source for these springs is likely geothermally
modified, old groundwater produced by water-rock
interaction at high temperature.

Electrical conductance measurements indicate high
amounts of dissolved solids, which also indicate high
water-rock interaction (Figure 10). The geothermal water is
likely deeply-circulating within the San Andreas Fault
System. The increase in electrical conductance and flow
rate also indicate that the water is being flushed out of
the system quickly (Figure 11).

Cold Springs in Ben and Sand Canyons

One spring in Ben Canyon, Site 157, exhibits
evaporative trends below the MWL (Figure 12). Mixing
calculations show that 80-93% of the spring's recharge is
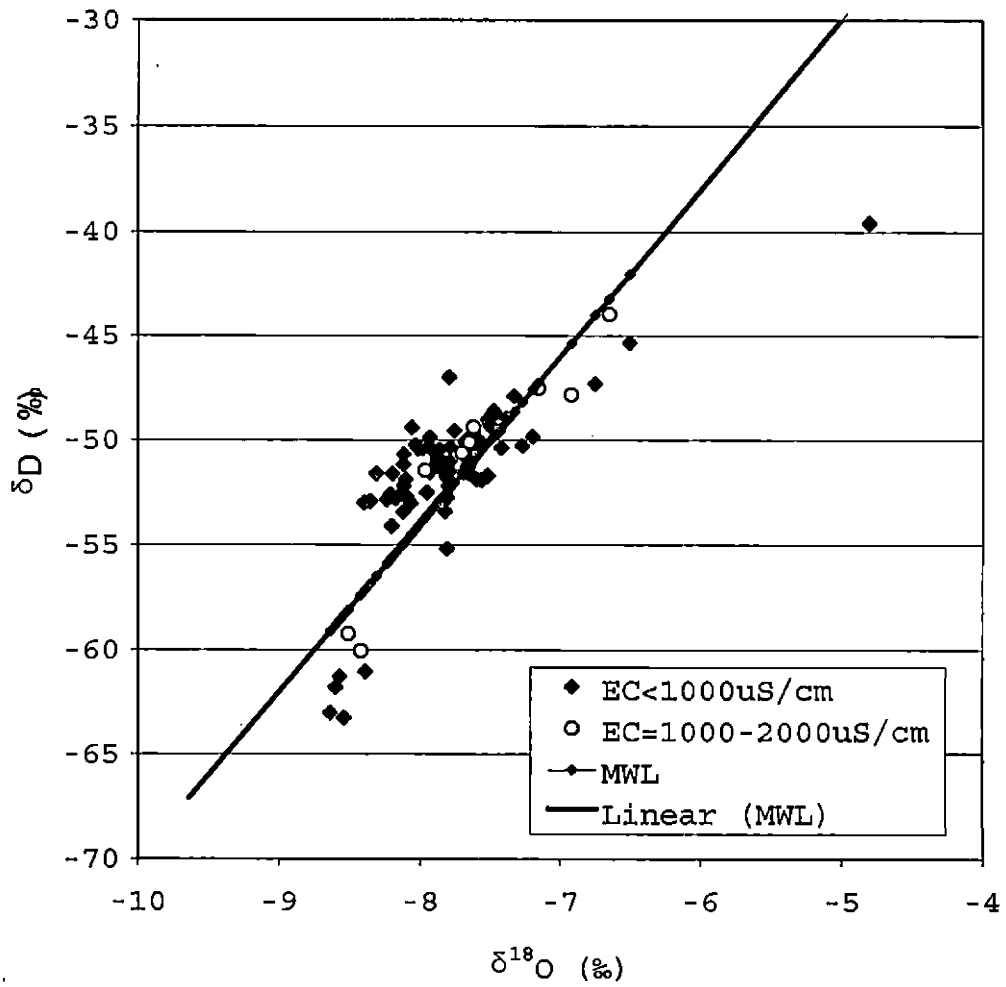meteoric in origin. This is indicative that evaporation is

41

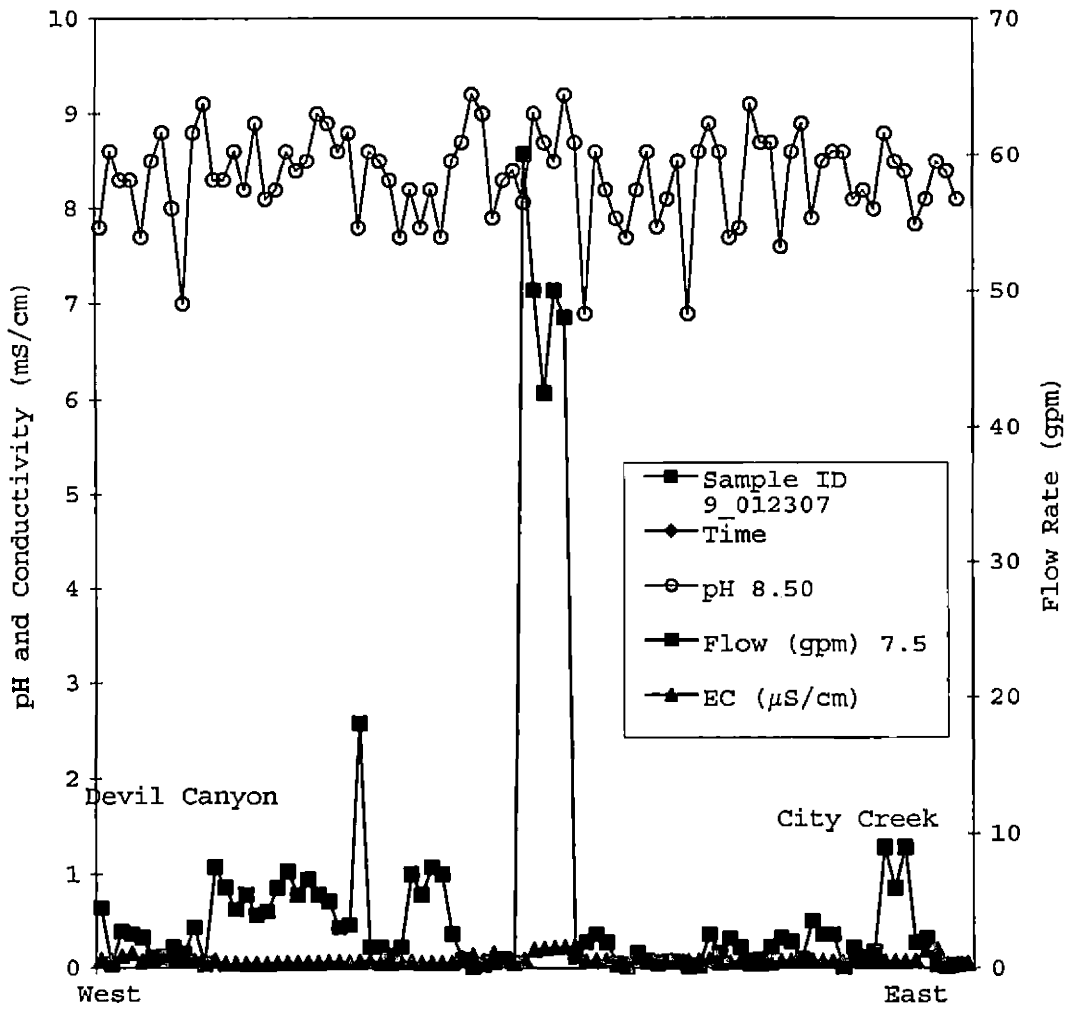Figure 10. Conductivity and Isotopic Values
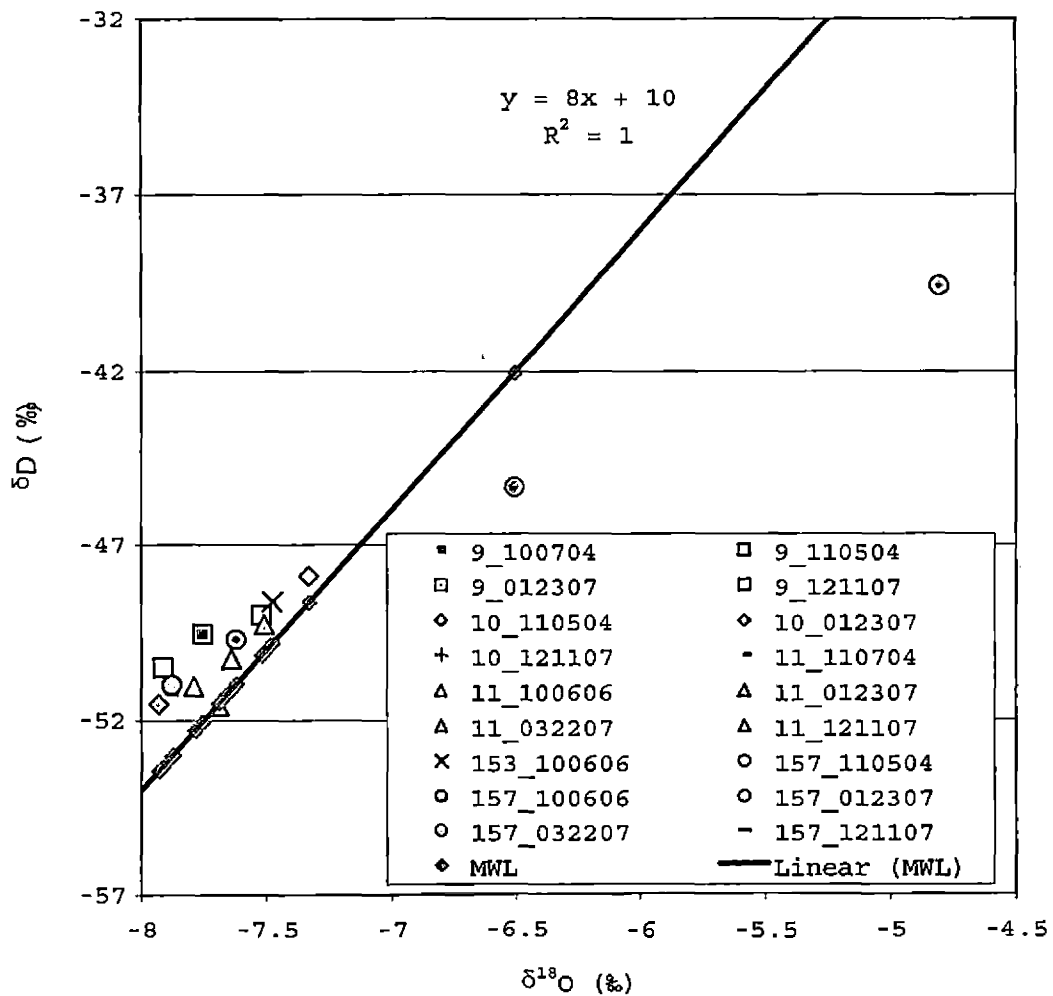
Figure 11. Flow Rate, pH, and Conductivity

Figure 12. Ben Canyon Isotopic Characteristics

occurring between the time of precipitation and the time of discharge. The recharge paths within the system could be long for spring 157, allowing for evaporation and the subsequent depletion in isotopic values. Faulting and jointing patterns in the canyon could be a cause for the long flow paths within the system, although the electrical conductance does not indicate long residence times.

Springs exhibiting isotopic values above the MWL suggest that the source of recharge could be snowmelt runoff from the mountains at higher elevations above the springs, which is consistent with the trends found by Izbicki et al. (1998) with snowmelt plotting above the MWL. Springs in both Ben Canyon (Sites 9, 10, and 11) and Sand Canyon (Sites 48 and 53) exhibit this effect, as shown in Figures 12 and 13. The low electrical conductance of the spring waters in these canyons is also representative of recharge sources that have not exchanged extensively with the geologic conditions (Figure 11).
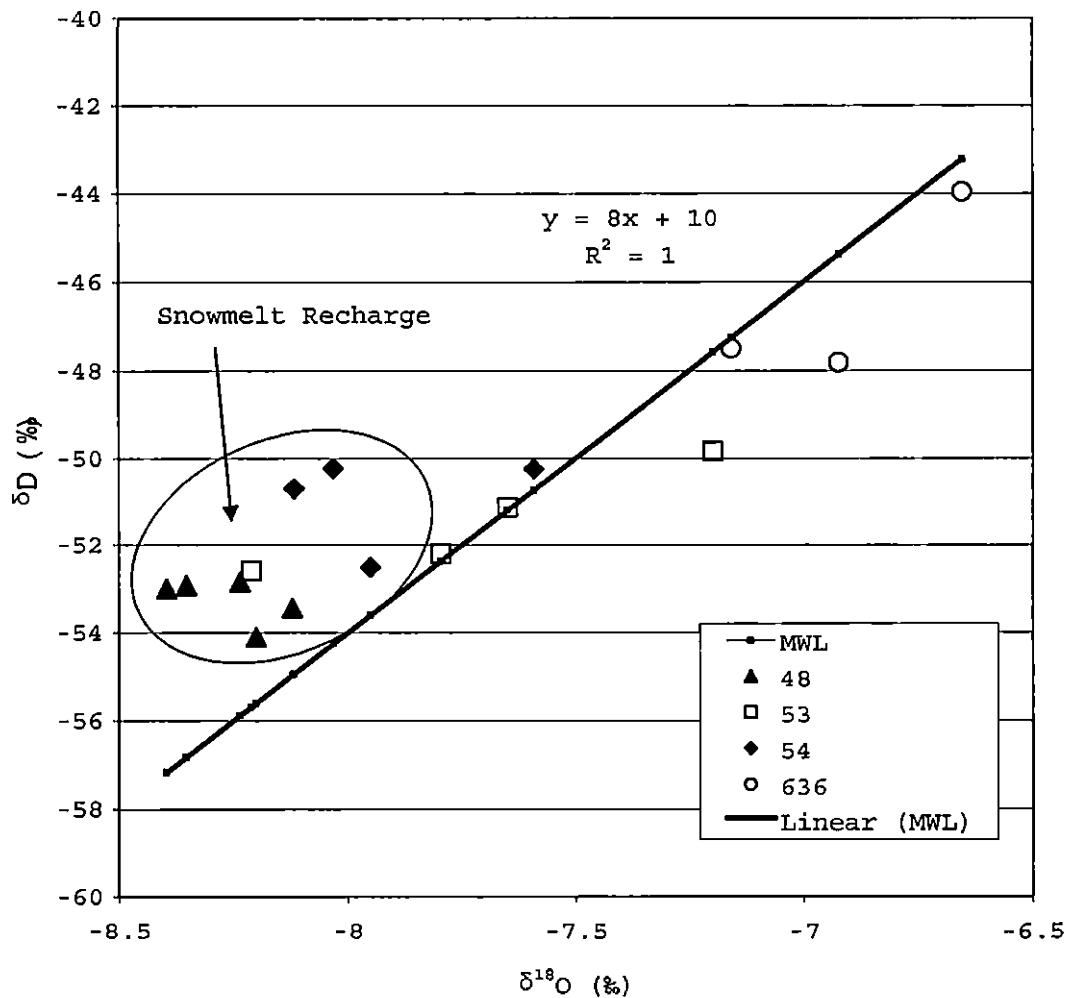
Figure 13. Sand Canyon Isotopic Characteristics

CHAPTER SIX

CONCLUSIONS

Conclusions

The results of all stable isotopic analyses, pH,
conductivity, water temperature, and flow rates indicate
that water recharging the springs in the San Bernardino
Mountains originates as recent meteoric precipitation,
recent snowmelt runoff, and old geothermal waters (Figure
14). The average change in isotopic composition is -0.59‰
per 1000 feet of elevation gain.

Geothermal waters appear to be the source of recharge
for hot springs occurring in Waterman Canyon, which is
bound by the San Andreas and Arrowhead Springs Faults. With
a range in values of $\delta^{18}O$ = -8.6 to -8.3‰ and δD = -63.2 to
-59.2‰, the geothermal waters plot well off the meteoric
water line, suggesting a source with high temperatures and
long residence time. Temperature, conductivity, and
isotopic measurements indicate that these hot springs
appear to have significant circulation at depth within the
San Andreas Fault System.

As meteoric water flows into a geothermal system via
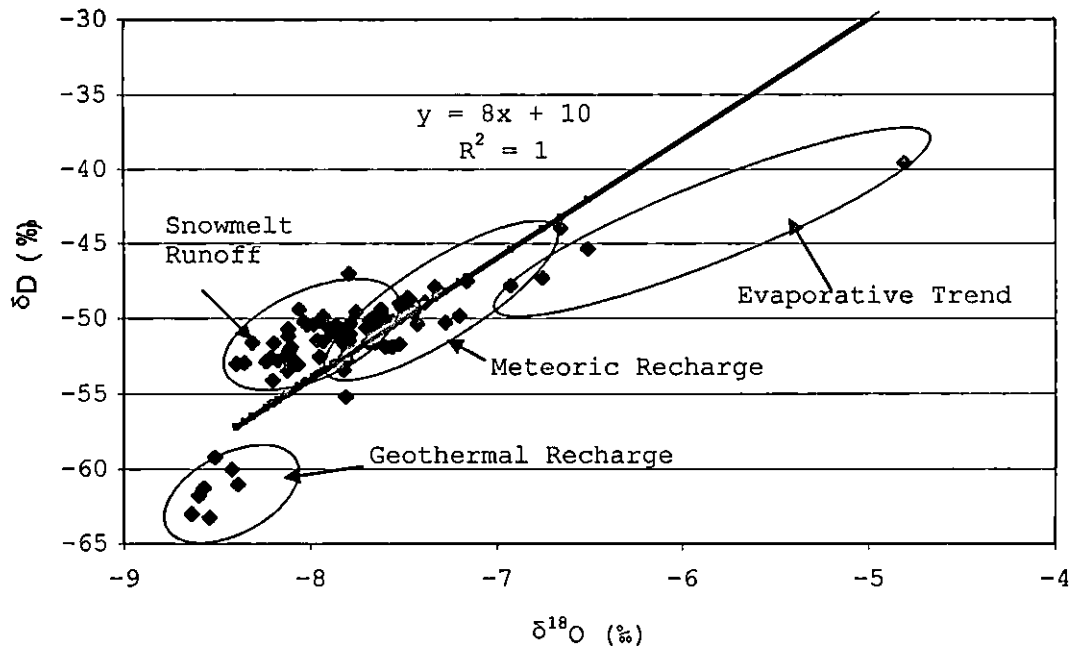fractures or faults and becomes heated, light meteoric

Figure 14. Sources of Recharge

oxygen and hydrogen exchange with heavier oxygen and hydrogen in the surrounding rock, causing a shift in isotopic values with heavier or more positive values. The high electrical conductance combined with the magnitude of the $\delta^{18}O$ shift in the water indicates the large amount of meteoric water that has exchanged with the rock. The δD shift is indicative of the amount of meteoric recharge water. Mixing calculations for the Waterman Hot Springs indicate that some mixing with meteoric water occurs (62% to 86%), with a substantial amount of water originating at a geothermal source.

Isotopic values plotting below the meteoric water line are indicative of evaporative effects occurring between the time of precipitation and discharge at the site. Mixing calculations for Site 157 in Ben Canyon exhibiting an evaporative trend show that 80-93% of the spring's recharge is meteoric in origin. Faulting and jointing patterns beneath the surface could cause long recharge paths, allowing for evaporation and subsequent depletion in isotopic values.

Snowmelt water runoff appears to be the source of recharge for many cold springs in Ben Canyon and Sand Canyon. Isotopic values plotting above the MWL are

consistent with those values measured in snowmelt runoff in previous investigations. As depleted snow falls at the higher elevations, the depleted runoff recharging the springs creates a depleted signature in spring water samples.

Meteoric waters appear to be the source of recharge for the remaining springs in the study area, as these values plot consistently along the MWL. Residence times may be slightly elongated by faulting, fracturing, and jointing in the subsurface hydrogeologic system.

Suggestions for Further Study

Although all 25 springs occur at similar elevations in similar geologic conditions, the range and variation of isotopic distributions within the study area leave some questions unanswered. More exact sources of recharge could be found for the cold water springs if snow samples collected above the study area and rain samples collected in and around the study area were analyzed and compared to the isotopic compositions of the spring discharge waters. With further study, a more exact source of geothermal water recharging the hot springs could be pinpointed using geothermometry data. Future studies of flow patterns and isotopic patterns combined with seismic data could be

useful in the interpretation of fault activity within the region. Understanding of the location and distribution of geothermal springs within these deeply fluid-supported segments within the San Andreas Fault System may assist future seismological studies.

APPENDIX A

MIXING CALCULATIONS

.

.

`

.

APPENDIX A
MIXING CALCULATIONS

642	1922	-7.3802
642	1922	-7.3802
157	2511	-7.9692

$\delta^{18}O_a = X_{MW} \; \delta^{18}O_{MW} + (1 - X_{MW}) \; \delta^{18}O_p$

Rearranged to produce:

$X_{MW} = (\delta^{18}Oa - \delta^{18}Op) / (\delta^{18}O_{MW} - \delta^{18}Op)$

XMW = amount of meteoric water

a = actual
p = predicted

Site	Canyon	Sample Date	Elev (ft)	δ18Oa	δ18Op	X_{MW}	%XMW
94	Waterman	10/11/2004	1954	-8.64	-9.40	0.62	62
94	Waterman	10/13/2006	1954	-8.54	-9.20	0.63	63
94	Waterman	1/19/2007	1954	-8.39	-8.80	0.70	70
94	Waterman	3/12/2007	1954	-8.57	-8.90	0.78	78
94	Waterman	12/10/2007	1954	-8.60	-8.90	0.80	80
642	Waterman	10/13/2006	1922	-8.51	-8.70	0.86	86
642	Waterman	12/10/2007	1922	-8.42	-8.80	0.73	73
157	Ben	10/6/2006	2511	-4.80	-4.00	0.80	80
157	Ben	3/22/2007	2511	-6.51	-6.40	0.93	93

REFERENCES

Abbott, M.D., Lini, A., and Bierman, P.R., 2000, $\delta^{18}O$, δD, and ^3H measurements constrain groundwater recharge patterns in an upland fractured bedrock aquifer, Vermont, USA, Journal of Hydrology, 228: 101-112.

Blasch, K.W., and Bryson, J.R., 2007, Distinguishing sources of ground water recharge by using δ^2H and $\delta^{18}O$, Ground Water, 45: 294-308.

Clark, I.D., and Fritz, P., 1997, Environmental Isotopes in Hydrogeology, Lewis Publishers, New York, 328p.

Craig, H., 1961, Isotopic Variations in Meteroic Waters, Science, 133: 1702-1703.

Dansgaard, W., 1953, The abundance of O^{18} in atmospheric water and water vapor, Tellus, 5: 461-469.

Dansgaard, W., 1954, The O^{18} abundance in fresh water, Geochimica et Cosmochimica Acta, 6: 241-260.

Dansgaard, W., 1964, Stable isotopes in precipitation, Tellus, 16: 436-468.

Danskin, W.R., McPherson, K.R., and Woolfenden, L.R., 2006, Hydrology, description of computer models, and evaluation of selected water-management alternatives in the San Bernardino area, California: U.S. Geological Survey Open-File Report 2005-1278, 178p. and 2pl.

Department of Water Resources, 2003, California's Groundwater Bulletin 118 Update 2003, 265p.

Epstein, S., 1956, Variations of the O^{18}/O^{16} ratios of fresh water and ice, National Academy of Science Nuclear Science Service, 19: 20-25.

Epstein, S. and Mayeda T.K., 1953, Variations on the $^{18}O/^{16}O$ ratio in natural waters, Geochimica et Cosmochimica Acta, 4: 213.

Faure, 1986, Principles of Isotope Geology, 2nd Edition, Wiley, New York, 589p.

Fournier, R.O., and Thompson, J.M., 1980, The recharge area for the Coso, California, geothermal system deduced from δD and $\delta^{18}O$ in thermal and non-thermal waters in the region, U.S. Geological Survey Open-File Report 80-454, 25p.

Friedman, I., 1953. Deuterium content of natural waters and other substances, Geochimica et Cosmochimica Acta, 4: 89-103.

Friedman, I., Machta, L., and Soller, R., 1962, Water vapor exchange between a water droplet and its environment, Journal of Geophysical Research, 67: 2761-2770.

Friedman, I., Redfield, Shoem, A. C., Harris, B. and Harris, J., 1964, The variations of the deuterium content of natural waters in the hydrologic cycle. Reviews of Geophysics, 2: 177-224.

Friedman, I. and Smith, G. I., 1970, Deuterium content of snow cores from Sierra Nevada area, Science, 169: 467-470.

Friedman, I. and Smith, G. I., 1972, Deuterium content of snow as an index to winter climate in the Sierra Nevada area, Science, 176: 790-793.

Friedman, I., Smith, G., Gleason, J., Warden, A, and Harris, J., 1992, Stable isotope composition of waters in southeastern California: 1. Modern precipitation, Journal of Geophysical Research, 97: 5795-5812.

Gat, J.R., 1980, The isotopes of hydrogen and oxygen in precipitation, In: P.Fritz and J.-Ch. Fontes (Eds.) Handbook of Environmental Isotope Geochemistry, Volume 1, The Terrestrial Environment, Elsevier, Amsterdam, p.21-48.

Hoefs, J., 1987. Stable Isotope Geochemistry, 3rd Edition, Springer-Verlag, 236p.

Ingraham, N.L. and Taylor, B.E., 1986. Hydrogen isotope study of large-scale meteoric water transport in

Northern California and Nevada., Journal of
Hydrololgy, 85: 183-197.

Ingraham, N.L., and Taylor, B.E., 1991, Light stable
isotope sytematics of large-scale hydrologic regimes
in California and Nevada: Water Resources Research,
127: 77-90.

Izbicki, J., Danskin, W., and Mendez, G., 1998, Chemistry
and isotopic composition of ground water along a
section near the Newmark area, San Bernardino County,
California: U.S. Geological Survey Water Resources
Investigation Report 97-4179, 27p.

Kendall, C. and McDonnell, J.J. (Eds.), 1998, Isotope
Tracers in Catchment Hydrology, Elsevier Science,
Amsterdam, 839p.

Magaritz, M., Aravena, R., Pena, H., Suzuki, O., and
Grilli, A., 1989, Water chemistry and isotope study of
streams and Springs in Northern Chile, Journal of
Hydrology, 108: 323-341.

Mayr, C., Lucke, A., Stichler, W., Trimborn, P., Ercolano,
B., Oliva, G., Ohlendorf, C., Soto, J., Fey, M.,
Haberzettl, T., Janssen, S., Schabitz, F., Schlesser,
G., Wille, M., and Zolitschka, B., 2007, Precipitation
origin and evaporation of lakes in semi-arid Patagonia
(Argentina) inferred from stable isotopes, Journal of
Hydrology, 334: 53-63.

Melchiorre, E.B., Criss, R.E., and Davisson, M.L., 1999,
Relationship between seismicity and subsurface fluids,
central Coast Ranges, California, Journal of
Geophysical Research, 104: 921-939.

Muir-Wood, R., and King, G., 1993, Hydrologic signatures of
earthquake strain, Journal of Geophysical Research,
98: 22,035-22,068.

Nathenson, M., Thompson, J.M., and White, L.D., 2003,
Slightly thermal springs and non-thermal springs at
Mount Shasta, California: chemistry and recharge
elevations, Journal of Volcanology and Geothermal
Research, 121: 137-153.

Paternoster, M., Liotta, M, and Favara, R., 2008, Stable isotope ratios in meteoric recharge and groundwater at Mt. Vulture volcano, southern Italy, Journal of Hydrology, 348: 87-97.

Rodoni, D., 1993, Stable isotopic variations of meteoric waters in southwestern California: A hydroclimatologic study, M.Sc. Thesis, Department of Geological Science, University of California, Riverside.

Rose, T.P., Davisson, M.L., and Criss, R.E., 1996, Isotope hydrology of voluminous cold springs in fractured rock from an active volcanic region, northeastern California, Journal of Hydrology, 179: 207-236.

Smith, G.I., Friedman, I., Gleason, J., and Warden, A., 1992, Stable isotope composition of waters in southeastern California: 2. Groundwaters and their relation to modern precipitation, Journal of Geophysical Research, 97: 5813-5823.

White, D.E., Barnes, I., and O'Neil, J.R., 1973, Thermal and mineral waters of non-meteoric origin, California Coast Ranges, Geological Society of America Bulletin, 84:547-560.

Williams, A.E., 1997, Stable isotope tracers: natural and anthropogenic recharge, Orange County, California, Journal of Hydrology, 201: 230-248.

Williams, A.E., Rodoni, D.P., and Lee, T.C., 1993, Hemet basin groundwater management program: isotopic investigation, Institute of Geophysics and Planetary Physics, University of California, Riverside Publication, IGPP/UCR-92/22.